UNIVERSIDADE DE SÃO PAULO

INSTITUTO DE FÍSICA
CAIXA POSTAL 66318
05389-970 SÃO PAULO - SP
BRASIL

PUBLICAÇÕES

IFUSP/P-1149

FOCAL PLANE DETECTING SYSTEM FOR THE SÃO PAULO TAGGER

R. Guarino, V.P. Likhachev and **M.N. Martins**
Instituto de Física, Universidade de São Paulo

Abril/1995

Focal Plane Detecting System for the São Paulo Tagger

R.Guarino, V.P.Likhachev and M.N.Martins

Laboratório do Acelerador Linear
Instituto de Física da Universidade de São Paulo, São Paulo, Brazil

Abstract

The tagging technique is briefly described and the main characteristics and parameters of both the spectrometer and the focal plane detecting system of the São Paulo tagger are presented, in order to discuss the use of the equipment at the low energy ($5 - 30\ MeV$) regime. The new photomultiplier tubes that will be used in the focal plane are described and the results of experimental tests simulating work conditions at low energies presented.

1. Introduction

Photonuclear reactions observables, in the near threshold region, have a sharp dependence on the photon energy, as indicated by theoretical calculations [1-3], leading to the necessity of precise knowledge of the photon energy in this kind of experiment.

Several methods were developed in order to get intense monochromatic photon beams [4-6]. After the development of high duty cycle electron accelerators, perhaps the most successful one is the tagging of bremsstrahlung photons with post-bremsstrahlung electrons by means of a magnetic spectrometer. The requirements placed upon a detecting system for this purpose are a high detection efficiency for electrons, a good time resolution (of about $1\ ns$), high energy resolution and a high count rate capability ($> 10^6\ Hz$).

The Physics Institute of the University of São Paulo is currently building a cw microtron with maximum energy of $E_o = 31\ MeV$ which, employing the tagging technique, will be able to deliver monochromatic photons in the

energy range of a few MeV to 28 MeV. This article describes briefly the tagging technique and presents the main characteristics and parameters of the focal plane detecting system of the São Paulo tagger, with emphasys in the low photon energy region. Estimatives of the main parameters and characteristics of the tagger were done based on theoretical calculations for the bremsstrahlung cross section and angular distribution and characteristics of the focal plane detectors determined experimentally by the simulation of work conditions at low energies.

2. General description

The bremsstrahlung tagging technique, illustrated in figure 1, is conceptually simple. A monochromatic electron beam with energy E_o incident on a thin radiator produces a continuous bremsstrahlung photon spectrum in the forward direction. Since the radiator is very thin (about 0.1% of a radiation length) the primary beam passes through the radiator practically undisturbed and is deflected by the magnetic spectrometer to the beam dump. A small fraction of the beam is scattered in the radiator, losing a significant part of its energy. The electrons that have final momenta in the acceptance range of the spectrometer are deflected to an array of detectors in the focal plane. The signal produced in one of those detectors, by an electron with energy E_{ri}, announces the presence of a photon with energy $E_{\gamma i} = E_o - E_{ri}$. A time coincidence between this signal and a signal from the nuclear reaction product detector indicates that the reaction was produced by a photon with energy $E_{\gamma i}$.

2.1. Spectrometer

The magnetic spectrometer [7] donated to the LAL by $MAX - Lab$, of Lund, Sweden, is a double-focusing inclined-plane-pole-faces type magnet (fig. 2). The dimensions of the magnet pole ($50 \times 25\ cm^2$) are so that the

flight-time difference between electrons with the same residual energy emitted inside the acceptance angle is less than 1 ns (the time resolution to be achieved).

The spectrometer has a solid angle acceptance of 60 msr ($\mid \theta_V \mid \leq 4^o$ and $\mid \theta_H \mid \leq 8^o$) and momentum acceptance of $\pm 20\%$ ($p_{max}/p_{min} = 1.5/1.0$).

2.2. Focal plane

The focal plane detectors are placed inside the same vacuum chamber of the radiator, thus eliminating windows that might cause energy losses or multiple scattering.

The system consists of an array of 22 plastic scintillators ($NE102A$) arranged in a ladder-like geometry (fig. 3). The scintillators are 18.6 mm wide (along the dispersion), 5 mm thick (along the electron path) and 50 mm high, joined to cylindrical light guides that bring the light out of the vacuum chamber onto photomultipliers tubes.

Dispersion value $D = \Delta/\delta$ $[cm/\%]$ varies from 0.52 at the beginning of the plane (where the low energy electrons arrive) to 0.92 at the end, where δ is the difference in energy (given in percentage of the central residual electron energy) and Δ is the distance in the horizontal direction, given in cm. The light collection efficiency of this arrange was measured to be about 25%. The energy resolution of the spectrometer, in this configuration, varies from 2.1% (at the beginning of the plane) to 0.95% at the end [7].

The system worked originally with $Philips - PM1911$ photomultiplier tubes and will work with $PEM - 87$ tubes, manufactured by the Kharkov Institute of Physics and Technology, Ucraine.

2.3. Characteristics of the $PEM - 87$ Tubes

The $PEM - 87$ tube has a semi-transparent $Sb - K - Cs$ photocathode, with working area of 314 mm^2, electrostatic focusing system and an eleven

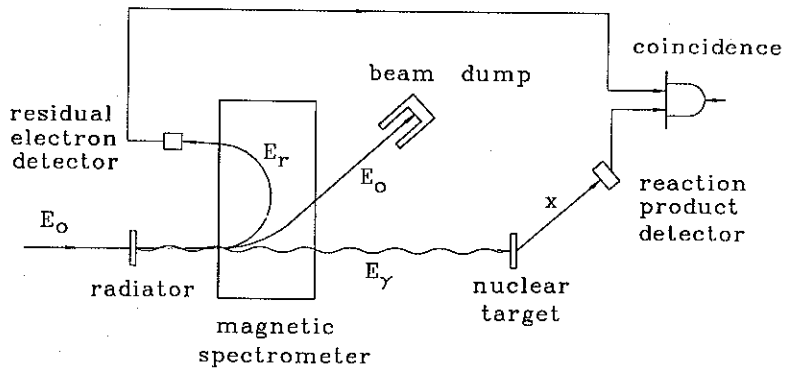

Figure 1: The schematic representation of photon tagging system with post-bremsstrahlung electrons

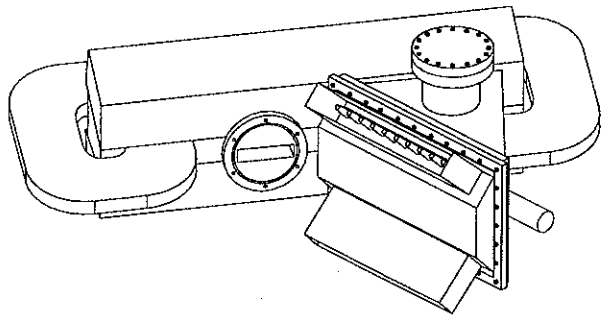

Figure 2: The magnetic spectrometer with the focal plane chamber

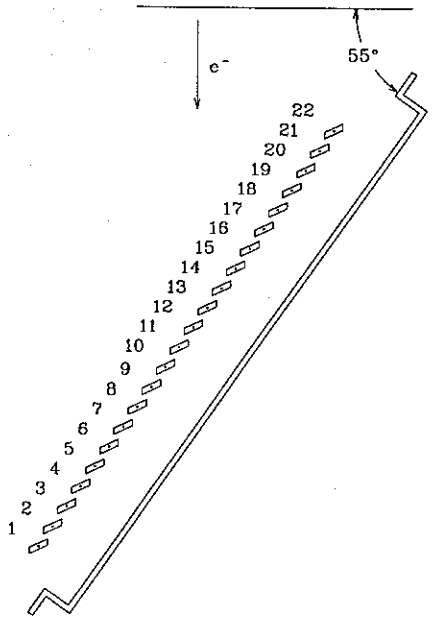

Figure 3: Top view of the focal plane detector array

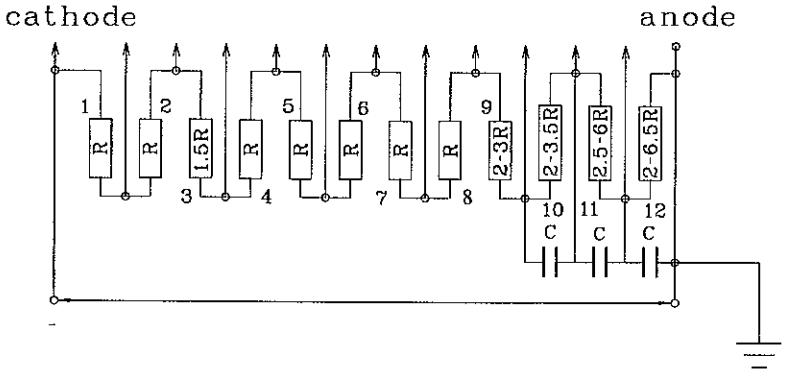

Figure 4: Schematic electronic circuit of the voltage divider

dynode cascade for electron multiplication.

The high voltage divider is uneven and the choice of resistances was done in order to optimize the anode pulse current (fig. 4). Since the equipment is expected to work under high count rate conditions, resistances $R = 75\ k\Omega$ were used in positions 1 and 2, and 4 to 8. Resistances numbers 3 and 9 to 12 were adjusted to achieve maximum signal output and signal-to-noise ratio. The power dissipation is $1W$ per resistance. The last three steps of the cascade were shunted with non-inductive capacitors in order to get an anode pulse with a full width at half maximum ($FWHM$) of about 5 ns.

The chosen photomultiplier (PM) tubes have high amplification coefficients so that we can work with not very high values of the high voltage, minimizing the divider current and thus getting good signal-to-noise ratio. All tubes will be fed by a single high voltage power supply. In order to avoid large variations in the signal amplitudes, the tubes were chosen with similar amplification coefficients and some of them received an additional variable resistor before the divider for fine tuning.

3. Coincidence rate

One of the most important parameters of a tagging system is the photon intensity, which is limited by two factors : finite count rate capability of the detectors and an acceptable level of random coincidences. The random coincidence rate between electron and product detectors is perhaps the main limiting factor. Even for an ideal case, where we consider 100% efficient detectors, 100% momentum acceptance for the tagger and the photon beam not collimated, such kind of limitation is still present. This limitation arises from what is called the ambiguity of tagging, the random coincidence between an electron and the detected nuclear product, since we have a much larger number of electrons arriving at the focal plane counters than reaction products on the other arm.

The bremsstrahlung process produces a continous photon spectrum K^{Br} with energies in the range $[0-E_o]$ as showed in figure 5. In an ideal case, each photon produced reachs the target and the product of the photoreaction is correlated to one electron detected in the focal plane. Random coincidences happen when the detected product and electron are not correlated. One cause of this is that the momentum acceptance of the spectrometer is less than 100%. In this case electrons with residual energy out of the spectrometer tagging interval are lost and the corresponding bremsstrahlung photons are untagged.

The count rate in the reaction product detector due to tagged photons is

$$N_x{}^{tag} = \frac{I}{e} N_{rad} N_{tar} \int_{E_1}^{E_2} \sigma_{\gamma x}(E_\gamma) K^{Br}(E_o, E_\gamma, Z) dE_\gamma \qquad (1)$$

and due to untagged photons is

$$N_x{}^{untag} = \frac{I}{e} N_{rad} N_{tar} \int_{E_3}^{E_4} \sigma_{\gamma x}(E_\gamma) K^{Br}(E_o, E_\gamma, Z) dE_\gamma \qquad (2)$$

where I is the beam current, N_{rad} (N_{tar}) is the number of atoms per cm^2 in the radiator (target), $\sigma_{\gamma x}(E_\gamma)$ is the cross section for photoproduction of particle x at the energy E_γ and $K^{Br}(E_o, E_\gamma, Z)$ is the bremsstrahlung spectrum produced by electrons of energy E_o striking a radiator with atomic number Z. In (1) the integration over photon energy is carried out in the range $[E_1, E_2]$ and in (2) the limits $[E_3, E_4]$ mean that the integration is carried out outside the tagging interval.

We have other limitations arising from the angular acceptance of electron and photon beams. The tagging efficiency is defined as the number of tagged photons, per energy interval, that reach the target, divided by the total number of counts in the focal plane detector which defines that interval. This value is reduced whenever the photon beam is collimated.

$$\varepsilon_t = \frac{N_\gamma}{N_e} \qquad (3)$$

In a first approximation these effects can be neglect because the scattering is concentrated around the incident beam direction.

The full count rate, N_e, in the tagging detector is equal to the number of electrons emitted into the solid angle of the spectrometer and within its momentum bite. The true coincidence rate, $N_{T,i}$, for the tagger counter i depends on the cross section for the photoproduction of particle x (see eq. 1), so

$$N_{T,i} = N_x{}^{tag} \qquad (4)$$

On the other hand, the total counting rate in the reaction product detector arises from tagged and untagged photons

$$N_x = N_x{}^{tag} + N_x{}^{untag} \qquad (5)$$

The random coincidence rate between the tagging and reaction product detectors will be approximately

$$N_{RC} = \frac{N_e\, N_x\, \tau}{D} \qquad (6)$$

where τ is the coincidence resolving time of the system and D is the macroscopic duty cycle of the accelerator. If the untagged photon rate (2) is raised, either due to limitation of the solid angle acceptance of the spectrometer or reduction of the tagging energy interval, the random coincidence rate is increased.

The ratio between true and accidental coincidence rates will be then

$$R = \frac{N_{T,i}}{N_{RC}} = \frac{N_x{}^{tag}}{(N_x{}^{tag} + N_x{}^{untag})} \frac{D}{N_e\, \tau} \qquad (7)$$

In the ideal case, with 100% momentum acceptance and very large solid angle, we have a full tagged interval and $N_x = N_x{}^{tag}$. Then the previous expression reduces to

$$R = \frac{D}{N_e\,\tau} \tag{8}$$

Supposing reallistic values for the duty cycle and resolving time of $D = 1$ and $\tau = 10^{-9}\ s$, we would get a count rate in the tagger limited to

$$N_e = \frac{10^9}{R}\ \ s^{-1}$$

The tagging efficiency (3) is less than unity and hence the tagged photon flux will also be limited by R:

$$N_\gamma \leq \frac{10^9}{R}\ \ s^{-1} \tag{9}$$

4. The choice of the working point

In order to simulate the focal plane conditions and test the PM-tubes we constructed a dark chamber to house the PM-tubes with a scintillator ($NE102A$), a support for radioactive sources and a light emitting diode (LED) for calibration.

The post-bremsstrahlung electrons arriving at the focal plane detectors of the tagger will deposit an energy of more than $1 MeV$ in the 5 mm thick scintillators. Since the light collection efficiency of the light guides is 25%, to simulate the focal plane detectors signal in our chamber we should have a 0.25 MeV source, because our scintillator is mounted directly onto the PM-tube, without light guide.

Using a ^{207}Bi source (conversion electron lines of 0.5 and 0.9 MeV) we calibrated our LED signals. Figure 6 shows the energy spectrum obtained with the LED simulating a 0.25 MeV electron signal. The count rate was

very low ($\sim 1\ Hz$) and one can see that we have a very good separation from the signal (peak around channel 250) and noise (small ramp on the left-hand side of the spectrum). Figure 7 shows the energy resolution of the PM-tube, the three peaks corresponding to electron signals of 0.1, 0.2 and 0.34 MeV respectively. The PM-tube energy resolution is better than 15%.

The working point was chosen so that the PM-tubes delivered signals of $-100\ mV$ amplitude for a 1 MeV energy deposition in the scintillator, so that we can use 50 mV threshold discriminators.

4.1. Count rate capability

We investigated the count rate capability of the PM-tubes using the LED. The minimum $FWHM$ of the pulses from the pulse generator was 30 ns, while real pulses from the scintillators will have $FWHM$ less than 5 ns and so the effect on the amplitude due to the increase in the counting rate should be less intense in the actual case.

Figure 8 presents the results obtained for the dependence of the anode pulse height on the frequency of the pulse generator, for three different initial signal amplitudes : $-60\ mV$ (crosses) ; $-100\ mV$ (squares) and ; $-150\ mV$ (triangles). It is clear from the figure that for the working amplitude of $-100\ mV$ the amplitude of the signal is stable up to a counting rate of $5 \times 10^6\ Hz$. In this case, each of the 22 tagger channels will be able to accept a count rate of this magnitude.

4.2. Time resolution

As mentioned above, the time resolution of the system should be of the same order or less than that of the flight-time difference of the electrons in the spectrometer (about 1 ns).

The PM-tube time resolution has two main components : time spread associated with amplitude spread (which is minimized by the use of constant

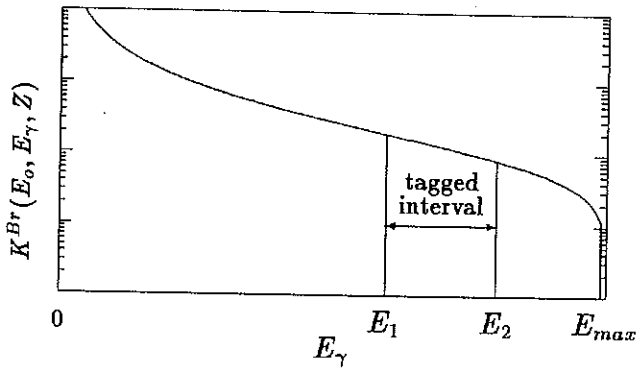

Figure 5: Typical cross section for bremsstrahlung production

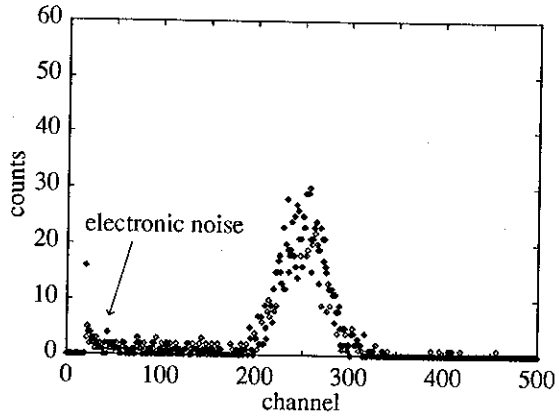

Figure 6: Energy spectrum from PM-tube obtained with a 0.25 MeV signal from a light emmiting diode

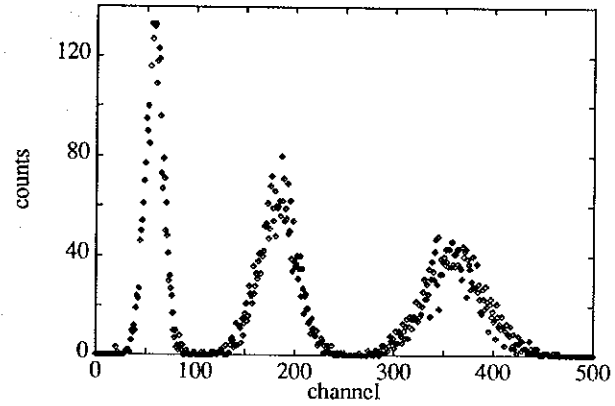

Figure 7: Energy resolution of the PM-tube

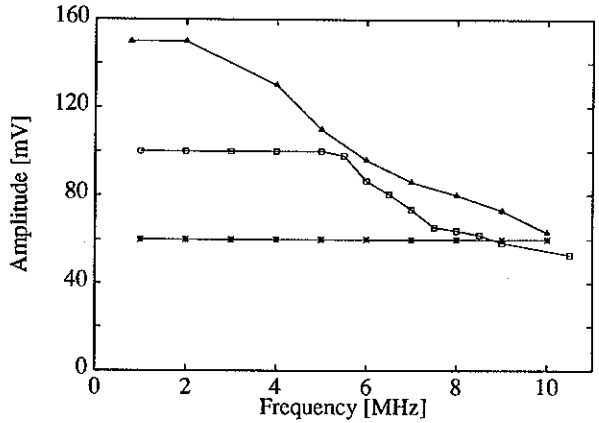

Figure 8: Amplitude as a function of the count rate

fraction discriminators) ; and intrinsic time fluctuation (*jitter*) of anode pulses of constant amplitude due to variations in the transit time of photoelectrons in the PM-tube during the multiplication process. This spread is a characteristic of the tube and cannot be reduced.

Figure 9 presents a time coincidence spectrum for the $PEM-87$ tube. The measurement was done splitting the pulses from the pulse generator in two (fig. 10). One pulse went through a delay line and constant fraction discriminator (CFD) to the *stop* input of the time-to-pulse-height-converter ($TPHC$), the other to the LED. The anode pulse from the PM-tube (triggered by the LED flash) was fed into a CFD and then to the *start* input of the $TPHC$. The coincidence spectrum was measured with anode pulse amplitudes of $-100\ mV$ to simulate the expected signals from electrons in the tagger. The $FWHM$ is about 1.5 ns, which comes from both the PM-tube and the LED *jitters*. So the PM-tube jitter is less than 1.5 ns, which is acceptable to our conditions.

The full time resolution of the system was measured in an electron-gamma coincidence (using a ^{207}Bi source). The experimental arrangement consisted of a $NaI(Tl)$ scintillator (2" $\times$ 2") and $RCA-8575$ PM-tube on the photon arm and a plastic scintillator ($NE102A, 4 \times 20\ mm^2$) and PM-tube $PEM-87$ on the electron arm. The source was put just beside the electron scintillator and at a few centimeters from the photon detector. There was no collimation of the source, so that the light collected by the PM-tubes came from the full volume of the scintillators. Constant fraction discriminators were used on both sides of the coincidence system. Figure 11 presents the time spectrum of the coincidences. The $FWHM$ of the peak is 3 ns, which is within the requirements of most planned experiments.

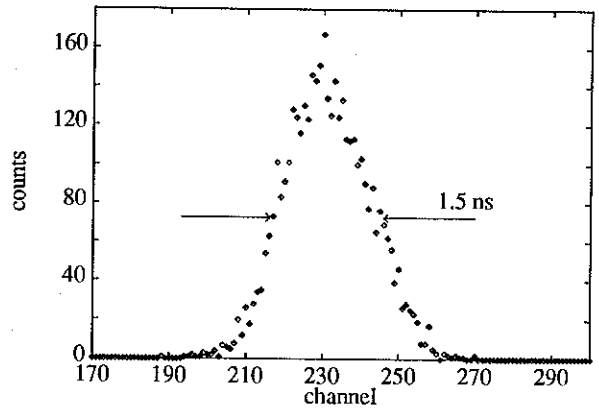

Figure 9: Time spectrum of the PEM-87 tube

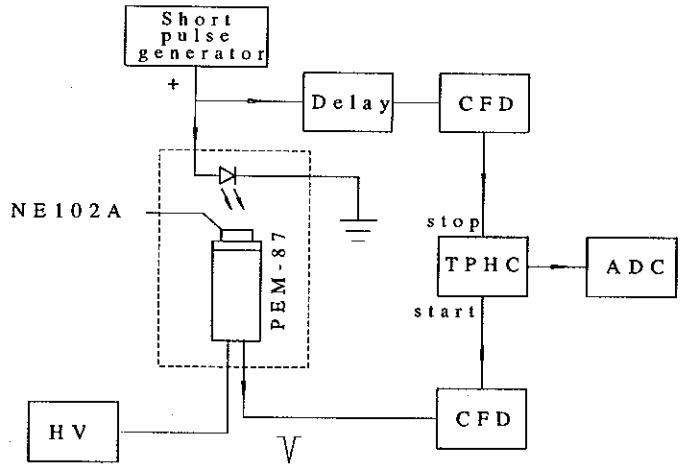

Figure 10: Block diagram of the time resolution measurement setup

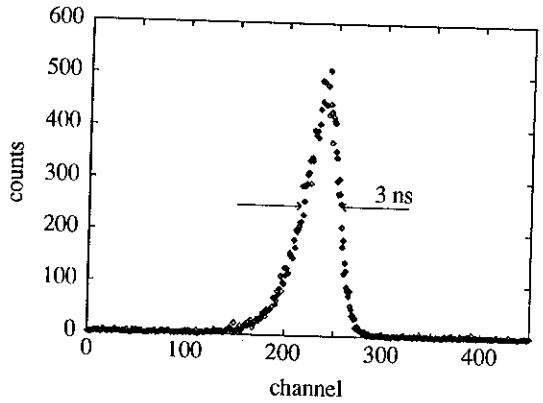

Figure 11: Time spectrum of the electron-gamma coincidences

5. Summary

The photon tagger detection system based on the $PEM-87$ photomultipliers meet the main requirements for the use at the low energy conditions of the São Paulo Microtron:

i. close to 100% efficiency for the detection of low energy electrons,

ii. high count rate capability ($5 \times 10^6\ Hz$ per channel),

iii. good time resolution (less than 1.5 ns).

The result for detection efficiency was obtained from measurements in simulated work conditions by a light emitting diode. The good separation between electronic noise and signal, showed in figure 6, assures that the noise can be eliminated without a significant loss of electron signal using constant fraction discriminators.

Our investigation on the count rate capability was performed with pulses from a pulse generator with 30 ns $FWHM$ (approximately 6 times the $FWHM$ from scintillators). Hence the maximum count rate of $5 \times 10^6\ Hz$ is underestimated.

A full time resolution of 3 ns was obtained with an electron-gamma coincidence system (fig.11). We expect to improve this by a factor of 2 optimizing the measurement conditions, that were far from ideal (poor ground and delay line).

6. Aknowledgements

The authors would like to thank the $MAX-Lab$ (Lund,Sweden), that gave us the electron spectrometer and the Kharkov Institute of Physics and Technology for the photomultipliers for the focal plane detection system. We would also like to thank $FAPESP$, $CNPq$ and $FINEP$ for the financial support.

7. References

1) A.J. Buki et al., Soviet Journal of Nuclear Physics 51(5)769-70,1990

2) N.A. Burkova, 'Cluster effects in the photodisintegration of light nuclei' in Proceedings of the 7th Seminar on Electromagnetic Interactions of Nuclei at Low and Medium Energies, Moscow, 1990, pp 234-247

3) Y.V. Vladimirov et al., Soviet Physics JETP 49(3)155-7,1989

4) L.S. Cardman, 'Photon Tagging' in Proceedings of the Magnetic Spectrometer Workshop, Williamsburg, 1983.

5) V.G. Gorbenko et al., Soviet Journal of Nuclear Physics 11(5)580-2,1970

6) R.M. Laszewski, P. Rullhusen, S. D. Hoblit and S. F. Lebrun, Nuclear Instruments and Methods 228, 334(1985)

7) J.O. Adler, B-E. Andersson, K.I. Blomqvist, B. Forkman, K. Hansen, L.Isaksson, K.Lindgren, D. Nilsson, A. Sandell, B. Schrder and K. Ziakas, Nuclear Instruments and Methods A294, 15(1990)